NUREG/CR-3230
MEA-2013

Effects of Temperature on Fatigue Crack Growth of a 508-2 Steel in LWR Environment

Prepared by W. H. Cullen/MEA
K. Torronen, M. Kemppainen/TRC

Materials Engineering Associates, Inc.

Technical Research Centre of Finland

ENSA, Inc.

**Prepared for
U.S. Nuclear Regulatory
Commission**

GPO Printed copy price: $4.50

NUREG/CR--3230

DE83 902017

Effects of Temperature on Fatigue Crack Growth of a 508-2 Steel in LWR Environment

Manuscript Completed: March 1983
Date Published: April 1983

Prepared by
W. H. Cullen, Materials Engineering Associates, Inc.
K. Torronen, M. Kemppainen, Technical Research Centre of Finland

Materials Engineering Associates, Inc.
9700 B George Palmer Highway
Lanham, MD 20706

Technical Research Centre of Finland
02150 Espoo 15, Finland

Under Subcontract to:
ENSA, Inc.
3320 Bailey Avenue
Buffalo, NY 14215

Prepared for
Division of Engineering Technology
Office of Nuclear Regulatory Research
U.S. Nuclear Regulatory Commission
Washington, D. C. 20555
NRC FIN B8133

GPO Printed copy price: $4.50

ABSTRACT

Fatigue crack growth rates were determined for A 508-2 steel in pressurized high-temperature, reactor-grade water, over a temperature range of 93°C to 288°C (200°F to 550°F). In addition, studies of the oxide layer on the fatigue fracture surface and of the fractography of these specimens were completed in order to provide information on corrosion-assisted, fatigue crack growth mechanisms. The crack growth data show a distinct minimum in growth rate at ~200°C (~400°F). Magnetite (Fe_3O_4) was found on the fatigue fracture surfaces at all temperatures. The fractography shows brittle-like features for all test temperatures. These observations suggest that hydrogen evolution may have occurred and that hydrogen-assisted crack growth may be responsible for the environmental effects observed.

CONTENTS

LIST OF FIGURES

ACKNOWLEDGEMENT

The author would like to acknowledge the efforts of Robert E. Taylor, MEA, and Craig L. Miller, ENSA, Inc., for assistance in conducting this research effort. The oxide examination was carried out by Dr. J. Atkinson of the Central Electricity Research Laboratory, Leatherhead, Surry.

Appreciation is also extended to Frank J. Loss, MEA, who provided program management covering most of this research.

1. EXECUTIVE SUMMARY

Fatigue crack growth rates have been measured for A 508-2 steel in pressurized water reactor (PWR) environments over a temperature range of 93°C to 288°C (220°F to 550°F). All other critical variables were held constant. The results indicate that a minimum in growth rate occurs at about 200°C. This agrees with other published work for A 533-B in a similar environment. The opposite effect, (i.e., a maximum in growth rates at about 20°C) has been noted for boiling water reactor (BWR) environments. For either case, the highest growth rates measured were at about the same level as the current ASME Boiler and Pressure Vessel Code guidelines found in Appendix A to Section XI.

For the present work on A 508-2, the oxide formed on the fatigue fracture surface was analyzed and a fractographic examination has been completed on specimens for four different temperatures. Magnetite alone was found on the fracture surfaces, indicating that the oxide formation mechanism is independent of temperature. Some characteristics of the fractography appear at all temperatures (brittle-like features and fan-shaped patterns), but ductile striations appear only at higher temperatures, while quasi-cleavage like features appear only at lower temperatures. All these facts taken together infer that two mechanisms may be responsible for these effects. One mechanism is active only at lower temperatures and becomes ineffective just below ~200°C. The second mechanism is active at all temperatures, but at higher ΔK values leads to increased crack growth rates with increasing temperature.

2. INTRODUCTION

The current positioning of the fatigue crack growth rate reference lines found in Appendix A of Section XI of the ASME Boiler and Pressure Vessel Code (Ref. 1) is based on a volume of crack growth rate data developed on several pressure vessel steels at 288°C (550°F). Continuing analysis of that volume of data, coupled with analysis of data from tests subsequent to the 1980 revision, has indicated that several critical variables have a predictive influence on crack growth rate. The effect of one of these important variables, load ratio, has been built into the code analysis (Ref. 2). The effects of other known critical variables have not yet been included. For example, the differences in boiling water reactor (BWR) and pressurized water reactor (PWR) environmental effects have not been separately accounted for, i.e., the reference line derivation was based on an amalgam of both kinds of data. This was justifiable in 1979, because relatively little BWR data were available, and they did show behavior similar to PWR data. The influence of sulfur content (Ref. 3) was based on examination of data sets for different heats of steel developed over several years of testing. This effect has since been confirmed by other laboratories (Ref. 4) and additional research is underway. The influence of waveform was described in 1979 (Ref. 5) and has also been confirmed by other laboratories (Ref. 4). The effects of irradiation have been found to be small, although the number of completed tests is also small and the data base needs to be expanded for additional safety assurance (Ref. 6).

In all these cases, the influence of these variables has been identified separately, since the delineation of combined effects requires a much larger test matrix, and consequently, longer testing schedules than are currently attainable. Ideally, a micromechanistic explanation of the crack tip and plastic zone processes is needed which accounts for these variations in crack growth rates. While various models are being developed (Ref. 7, 8), all are far from the applications stage. Meanwhile, work on identification of separate variables must continue both for reassurance that the code default lines are reasonable and for input to the models which are under development.

During start-up, the reactor wall temperature rises from 90-100°C to the operating level of 288°C. As a consequence, it is necessary to determine the fatigue crack growth rates in pressure vessel materials as a function of temperature, and some data addressing this point have been previously published. In 1973, Kondo, et. al. published A 302B data from tests using fully-reversed, strain-controlled cycling of precracked tension bars (Ref. 9). The environment was deionized water with about 200 ppb dissolved oxygen. Prater and Coffin have more recently published results for SA 333 Gr.6 piping steel in highly oxygenated water (Ref. 10). For PWR environments, Atkinson et al. have published results for A 533B (Ref. 11). Some of the initial results for this present study were presented at the ASME-PVP meeting in 1982 (Ref. 12). In parallel with the present fatigue crack growth rate studies, research has been conducted on oxide formation and corrosion potential measurement as functions of temperature. This current

study describes an attempt (a) to characterize fatigue crack growth rates as a function of temperature, and (b) to suggest the micromechanistic cracking processes which are responsible for the environmentally-assisted behavior of the fatigue crack growth rates, based on oxide identification and fractography.

3. MATERIALS

Compact fracture specimens (1T-CT) in the TL orientation were machined from a reactor vessle nozzle drop-out. The material chemistry and mechanical properties are given in Table 1. All specimens were precracked in air with a final K_{max} of 16.2 MPa $\sqrt{m}$ (14.7 ksi $\sqrt{in}$) at a load ratio (R) of 0.1.

Table 1. Material Chemistry, Heat Treatment, and Tensile Strength For A508-2 (Q71-code)

C	0.19	
Mn	0.69	Austentized at 840°C (1550°F) for 9h,
P	0.007	water quenched, tempered at 650°C
S	0.009	(1210°F) for 12h, air cooled; stress
Si	0.31	relief annealed at 660°C (1225°F) for
Ni	0.82	20h, furnace cooled 30°C/h max) 55°F/h
Cr	0.38	max).
Mo	0.62	
Cu	0.01	
V	0.13	

0.2% offset yield strength:		Ultimate tensile strength:	
MPa	(ksi)	MPa	(ksi)
538	(78.0)	680	(98.6)
555	(80.5)	692	(100.4)

4. TEST PRACTICE

On a laboratory scale, these tests are carried out in autoclaves which simulate reactor conditions in terms of temperature, pressure, and water chemistry. Each specimen is instrumented with a displacement gage for measuring crack mouth opening, δ. The load (P) is monitored by a load cell external to the autoclave chamber. The current crack length (a) is computed from an experimental relation between crack length and compliance (EB δ/P). At the beginning of a test, the crack length as inferred from the compliance, is corrected by adjusting the compliance used in this calculation to be consistent with the optically measured surface trace of the fatigue precrack. At the conclusion of a test, the initial and final crack lengths, measured optically, are compared with those computed from compliance. Small discrepancies, which in this series of tests ranged from -0.2 to +0.75 mm, are reconciled by rescaling the compliance data with the error correction applied in proportion to the cyclic count for each compliance measurement. Correct crack lengths are computed from these rescaled compliance values.

The tests were conducted under constant cyclic load control, and in two parts. For both parts of all tests, the load ratio was 0.2, which precluded effects of crack closure due to oxide wedging or other effects. The first part consisted of cycling at 1 Hz and extending the crack from 15.2 mm (0.6 in) to 20.3 mm (0.8 in.) covering a ΔK range from about 15.5 to 18.5 MPa $\sqrt{m}$ (14 to 17 ksi $\sqrt{in}$.). This part of the test represents an attempt to stabilize the environment-material interaction within the crack tip enclave, while at the same time extending the crack to a length at which the specimen compliance-to-crack length relationship is more sensitive, thus improving the accuracy of the data acquisition. The second part of the test consisted of cycling at 17 mHz (20 mHz in the case of specimen Q71-15) and extending the crack at the same loads as for the first part, to a final length of about 33 mm (1.3 in.). The final ΔK was about 55 MPa $\sqrt{m}$ (50 ksi $\sqrt{in}$.). Test temperatures were 93°C, 149°C, 204°C and 288°C, (200°F, 300°F, 400°F, and 550°F).

In order to accurately simulate the pressurized water reactor coolant environment, the water in the test system is carefully monitored and regulated to yield the specfications shown in Table 2. Water is deoxygenated by continuously bubbling hydrogen gas through the contents of the feedwater tanks.

Table 2. Water Chemistry Specification[a]

Boron (as boric acid)	1000	ppm
Lithium (as lithium hydroxide)	1	ppm
Chloride ions	<0.15	ppm
Fluoride ions	<0.10	ppm
Dissolved oxygen	~1	ppb
Dissolved hydrogen[b] (saturation)	30-50	cm^3/kg water

[a]All other metallic or ionic species should be at trace levels. Some iron, both in solid and soluble form is the inevitable result of a corroding specimen.

[b]For the test of Q71-24, the water was saturated with nitrogen instead of hydrogen

5. RESULTS AND DISCUSSION

5.1 Fatigue Crack Growth Rates

The fatigue fracture faces from representative specimens tested at the four temperatures are shown in Fig. 1. Crack extension was even and curvature was uniform for all the tests. The oxide was a lighter grey at 93°C, tending toward black at the higher temperatures, and appeared to be tightly adherent at all temperatures.

A graph of crack length vs. cyclic count for these tests is shown in Fig. 2. It is obvious that total test duration increased monotonically with temperature. However, the slopes of the traces for the tests conducted at 204°C are significantly different than the other slopes. This leads to significantly lower crack growth rates at 204°C, as described below.

The fatigue crack growth rate results for this series of tests are shown in Figs. 3 to 6, beginning with the lowest temperature results. For comparison, fatigue crack growth rate results in an air environment, at 288°C are shown in Fig. 7. At 93°C, specimen Q71-24 was tested in a slightly pressurized (35 kPa, 5 psi) test chamber using nitrogen gas saturated water, specimen Q71-25 was tested in a fully-pressurized autoclave (13.7 MPa, 2000 psi) for which the feedwater (275 kPa, 40 psi) was saturated with hydrogen (Fig. 3). The goal of this comparison was to eliminate test device and purging gas as potential variables in this study. The replicate test at a temperature of 204°C was run to confirm the substantial decrease in crack growth rates at that temperature (Fig. 5).

The notable characteristics of this test series are described below.

1. The growth rate results at 204°C differ substantially from the others in the nature of their dependence on ΔK. At the higher ΔK values, a "plateau" region exists where growth rates are essentially constant or independent of ΔK.

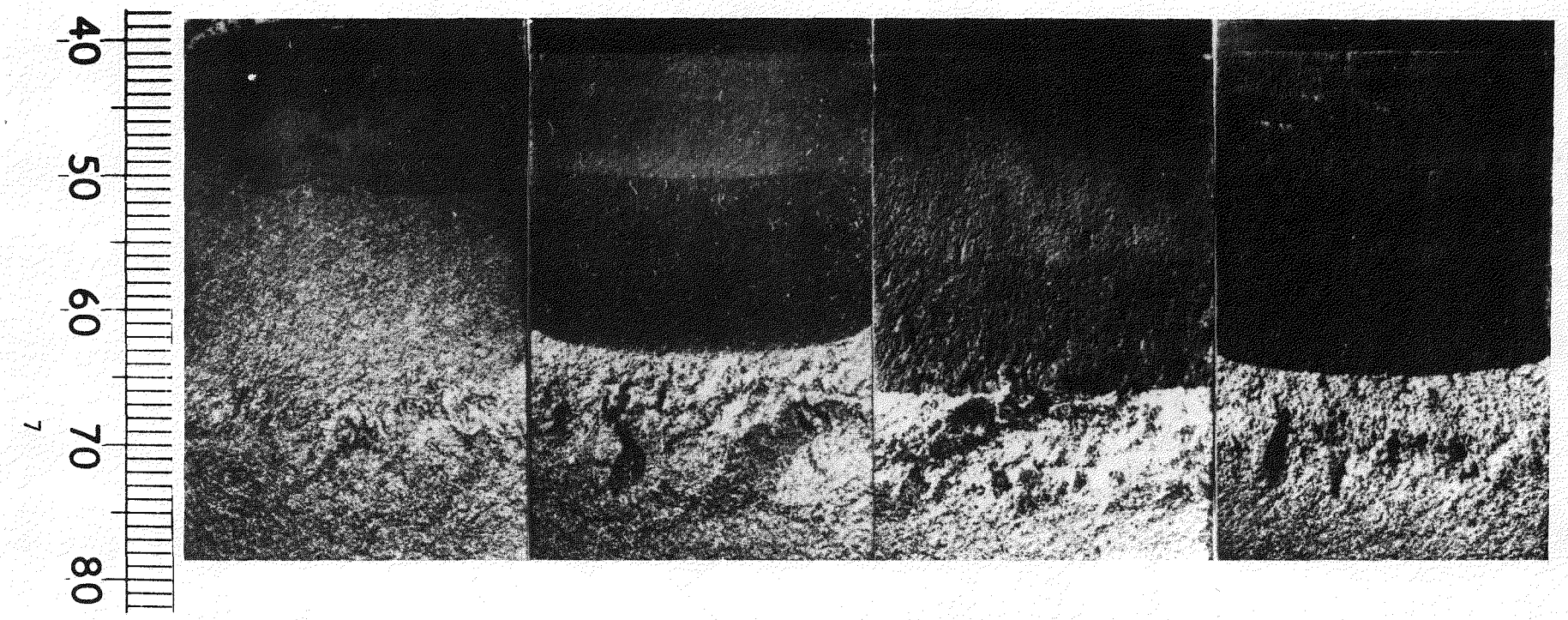

Fig. 1. Macrophotographs of four of the specimens which were tested for this study, and which were examined for oxide on the fatigue fracture surface, then stripped and examined fractographically

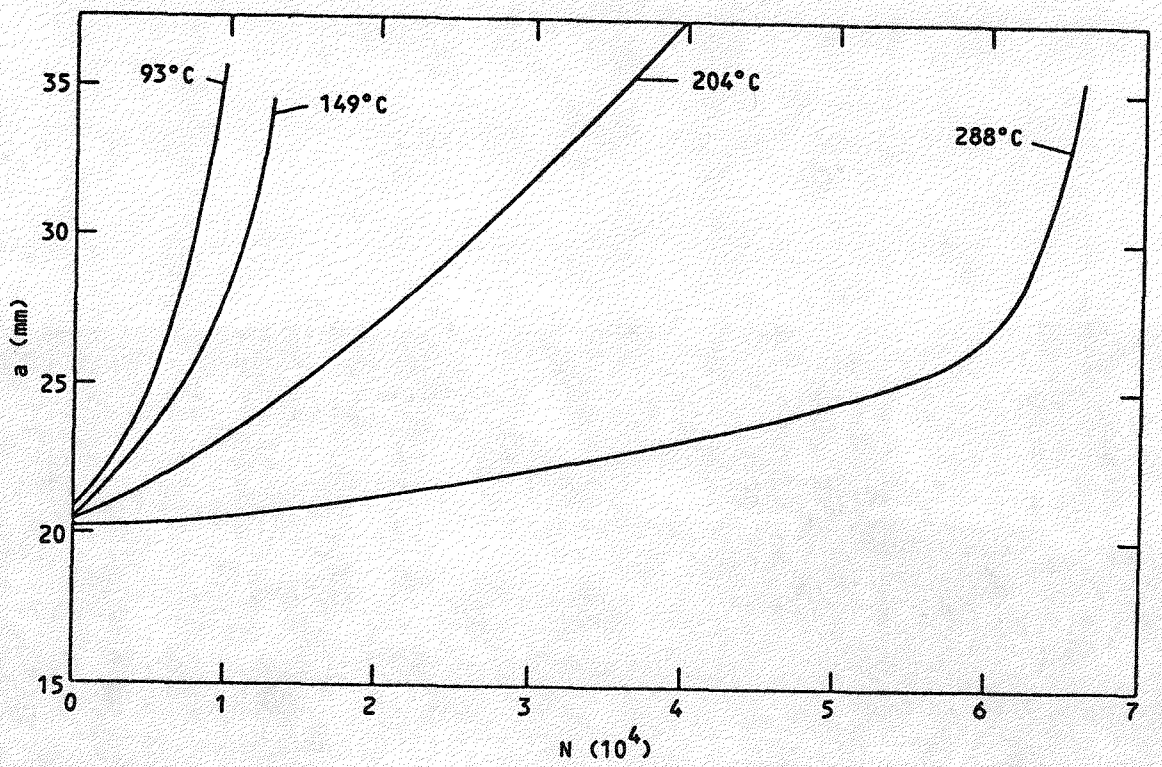

Fig. 2. Crack extension vs. cyclic count of the specimens tested for this study. Note the essentially monotonic increase in test time with increasing temperature. However, the slope of the tests at 204°C differs markedly from the balance of the tests at other temperatures, and this is reflecte in the crack growth rate plots of Figs. 3 to 6.

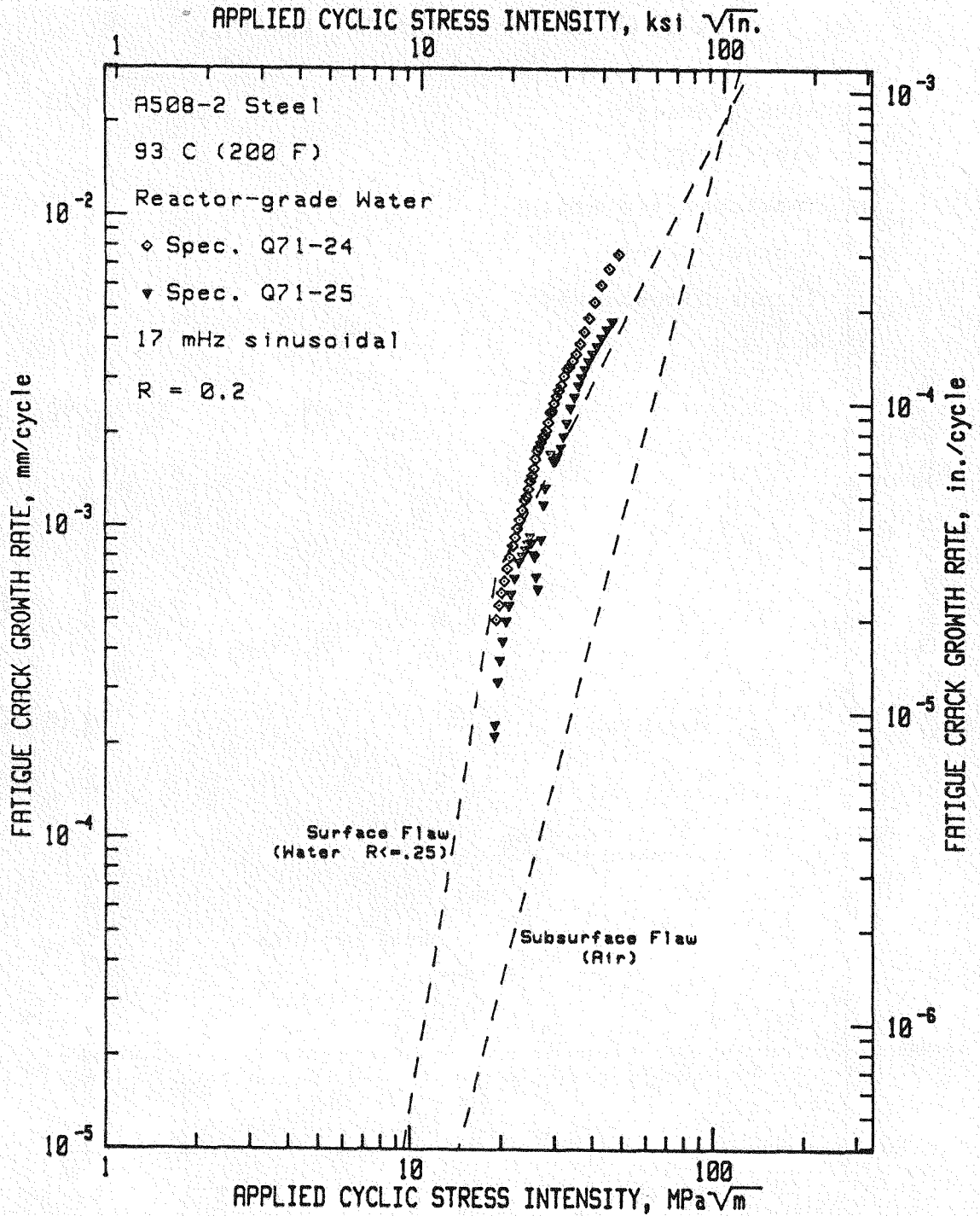

Fig. 3. Fatigue crack growth rates vs. applied cyclic stress intensity factor for two specimens of A 508-2 tested at 93°C (200°F). These specimens were tested in two different test facilities, to evaluate any systematic differences due to the materials of construction of an autoclave, and due to the purging gas (hydrogen Q71-25) and nitrogen (Q71-24) used in these facilities. Note the basically linear behavior.

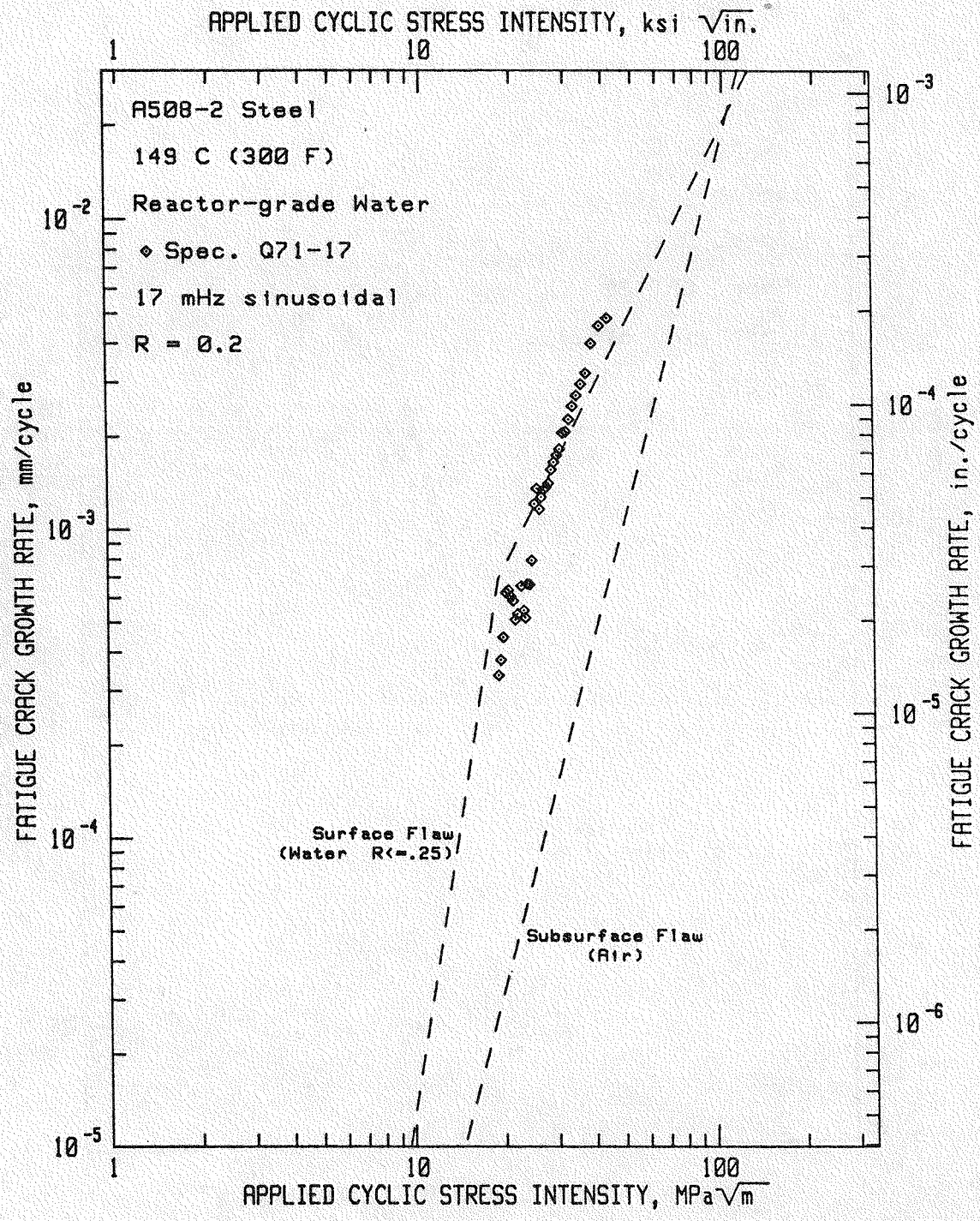

Fig. 4. Fatigue crack growth rates vs. applied cyclic stress intensity factor for A 508-2 tested at 149°C (300°F). As in the lower temperature test, the behavior is basically linear.

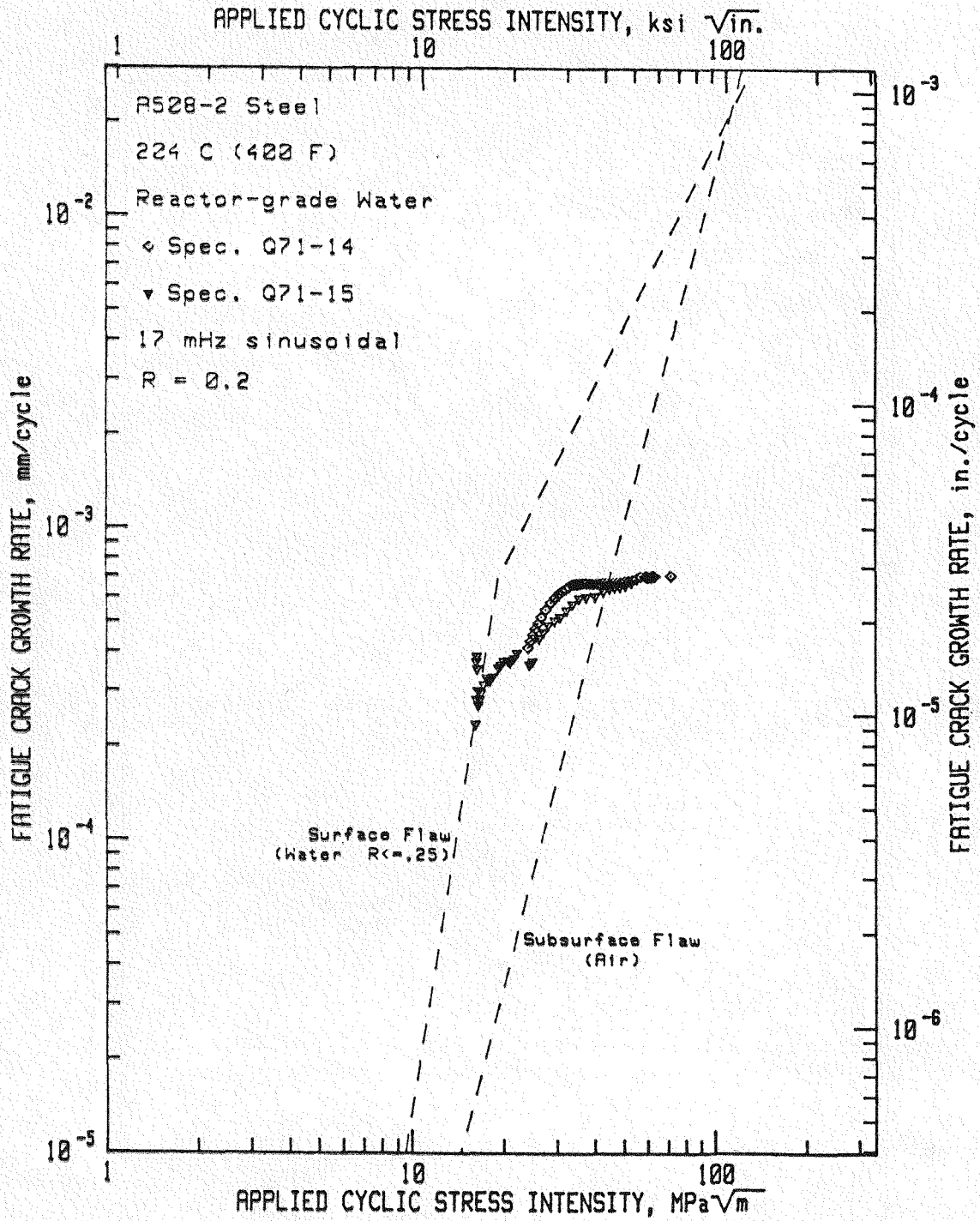

Fig. 5. Fatigue crack growth rates vs. applied cyclic stress intensity factor for two specimens of A 508-2 tested at 204°C (400°F). Note the distinct "plateau" region and overall lower growth rates at this temperature.

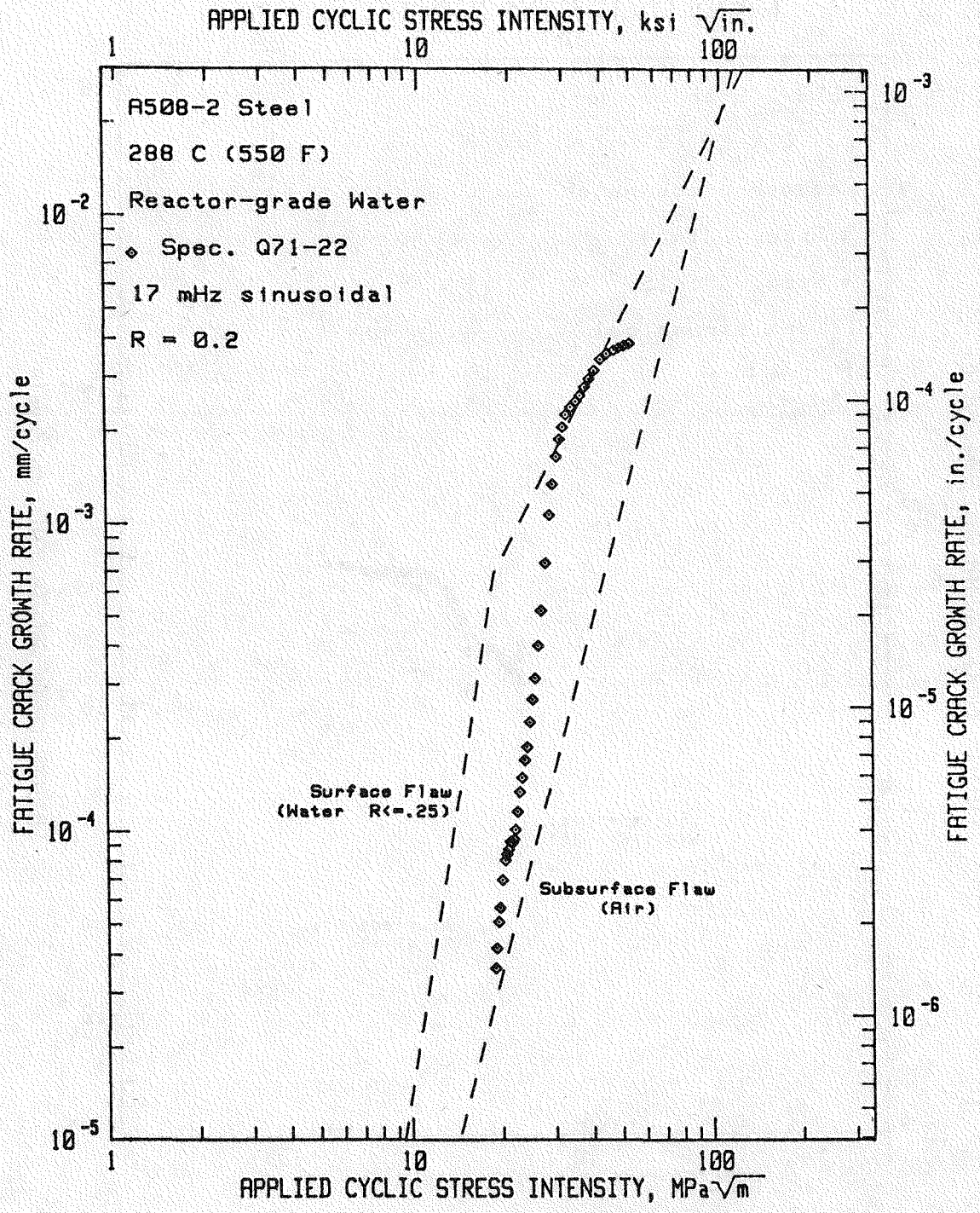

Fig. 6. Fatigue crack growth rates vs. applied cyclic stress intensity factor for A 508-2 tested at 288°C (550°F). The "bend-over" at the higher ΔK appears to be the onset of a plateau although growth rates at this temperature are higher than at 204°C.

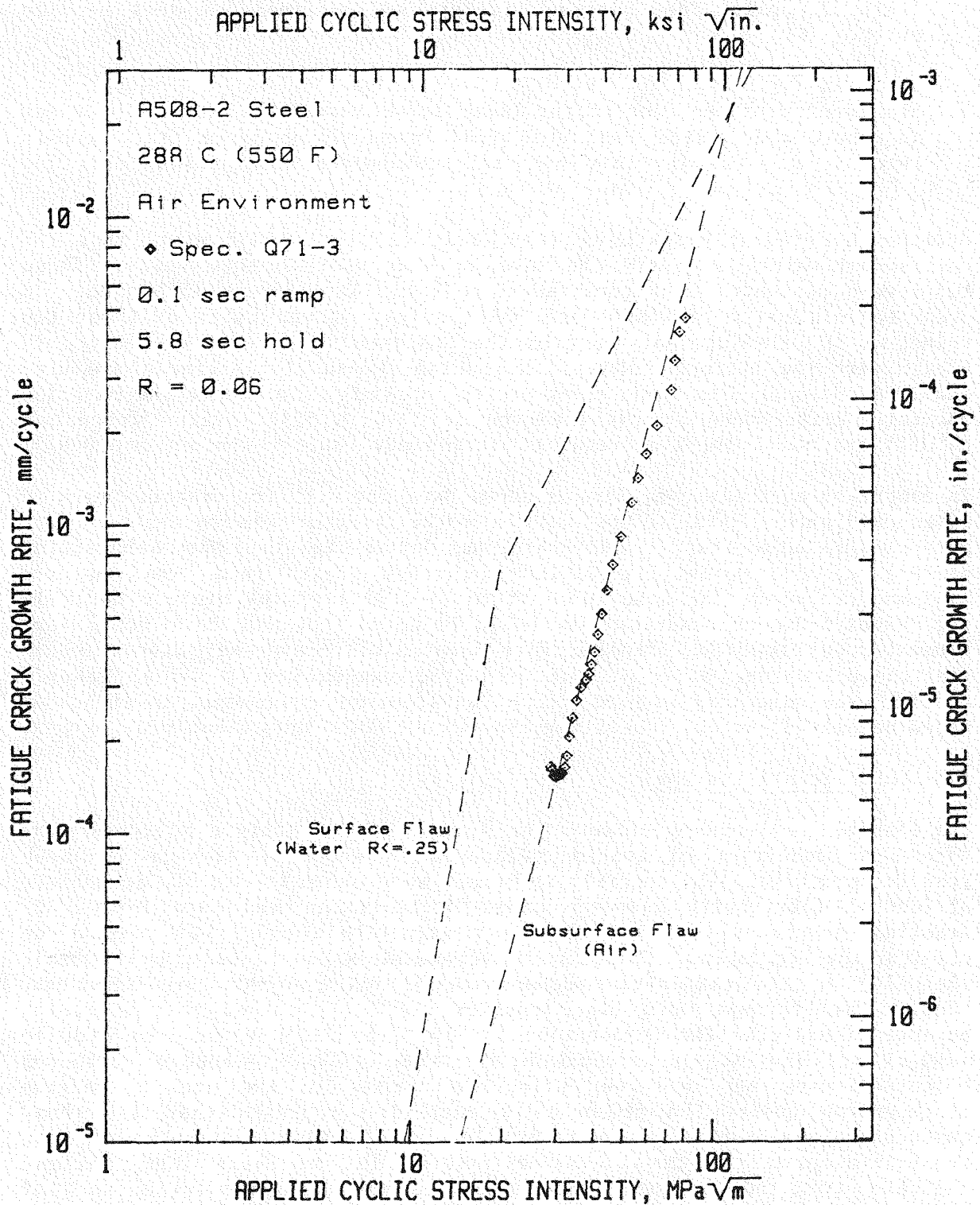

Fig. 7. Fatigue crack growth rates vs. applied cyclic stress intensity factor for a 288°C air environment test.

2. The growth rate results at 288°C show a "bend-over" at the higher ΔK values, in agreement with a large volume of previously published data (Refs. 2,6,13). The "plateau" is less well-defined but does seem to exist.

3. The results of the test at the lower temperatures are basically linear in nature and reside near the upper bound of measured crack growth rates at R = 0.2 for this material-environment combination (Ref. 2).

Atkinson has recently published data (Ref. 11) for A 533B steel in a PWR environment which is nearly the same as that used in this study. Those tests were conducted in a constant ΔK mode for ΔK = 35 and 45 MPa $\sqrt{m}$. In order to compare the Atkinson and MEA results, growth rates at those two values of ΔK were interpolated from the MEA results and are co-plotted in Fig. 8 with the Atkinson data. The general shapes of the trends are virtually identical. The lower crack growth rates might be due to the material chemistry differences in the Atkinson test of A 533B (sulfur content = 0.005%) and the A 508-2 material of this study (sulfur content = 0.009%).

In contrast, to the above, Fig. 9 shows data for high-temperature tests in oxygenated water, similar to boiling-water reactor environments. Data generated by Kondo (Ref. 9) and Prater and Coffin (Ref. 10) show substantial difference, most notably, a maximum in crack growth rates was observed by Kondo, at about the same temperature (~ 200°C) of the minimum noted in the PWR-environment studies. It should be noted that the Kondo tests were conducted on precracked tension bars under fully-reversed, displacement-controlled loading, at a 200 ppb dissolved oxygen level, while Prater's results were generated on more conventional compact specimens, in air-saturated deionized water, resulting in about 8000 ppb dissolved oxygen.

5.2 Oxide Identification

The elevated-temperature oxide layer formed on the fatigue fracture surfaces was identified on specimens exposed in water at each of the four test temperatures. The specific specimens were shown in Fig. 1. Scientists at Central Electricity Research Laboratories-Leatherhead used X-ray diffraction techniques and concluded that magnetite (Fe_3O_4) was present on all fracture surfaces. This is in agreement with a study by McDonald (Ref. 14) of the temperature dependence of oxide product on low-carbon steel. The Atkinson work cited earlier (Ref. 11) showed that corrosion potentials measured for temperatures of 150°C to 290°C range from -650 to -850 mV vs. the standard hydrogen electrode (SHE). Although corrosion potentials were not measured during the course of the present fatigue crack growth tests, the presence of magnetite suggests that for these tests also the potentials were rather low (<-600 mV). With reference to a Pourbaix diagram for the ironwater system, it is likely that hydrogen evolution from the fatigue fracture surface was occurring during each of these tests.

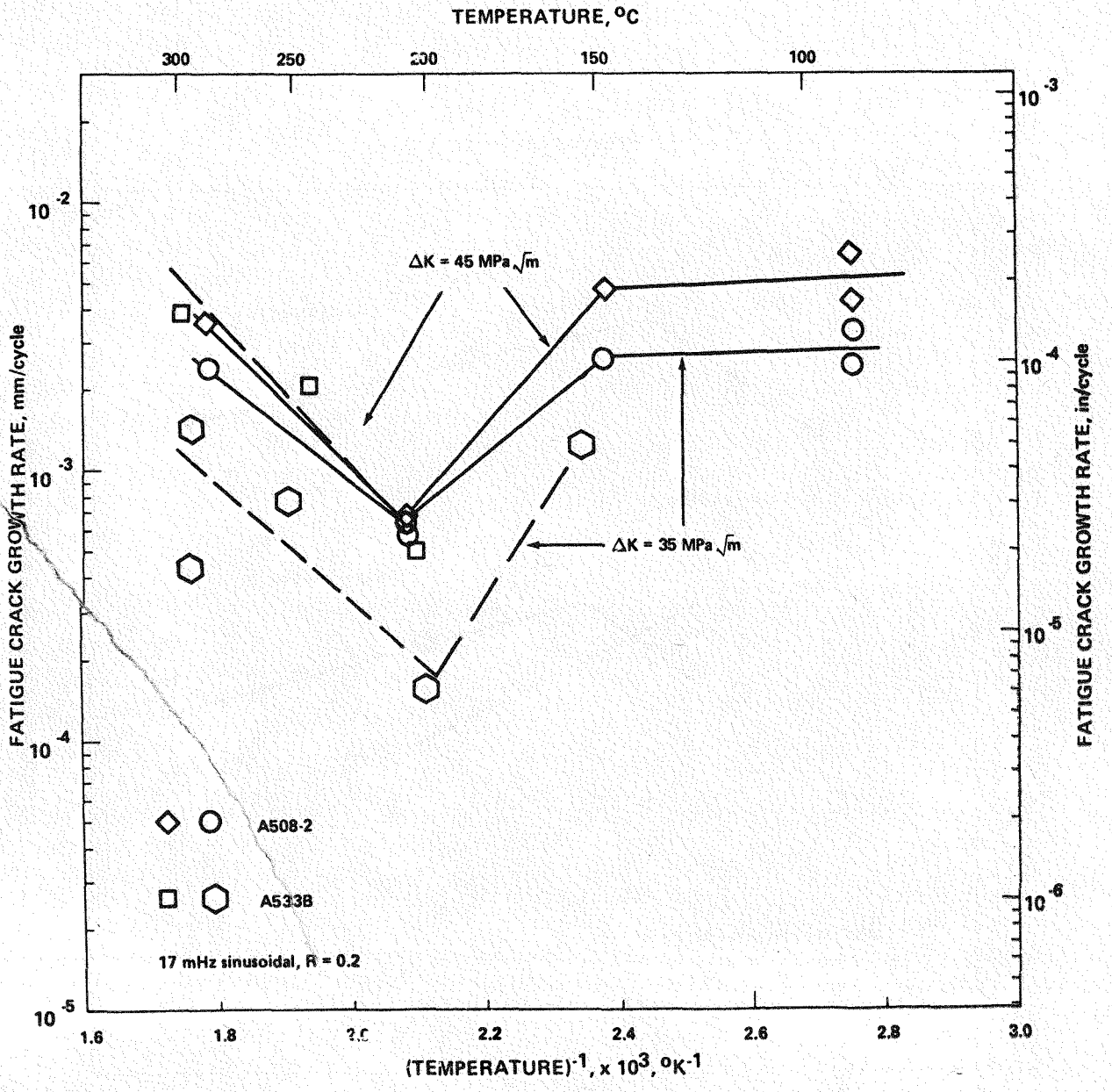

Fig. 8. Fatigue crack growth rates of A 508-2 and A 533 B at specific values of ΔK vs. reciprocal temperature, for PWR environments, showing that growth rates are minimized for temperatures near 200°C. The data for A 533-B are taken from Atkinson (Ref. 9).

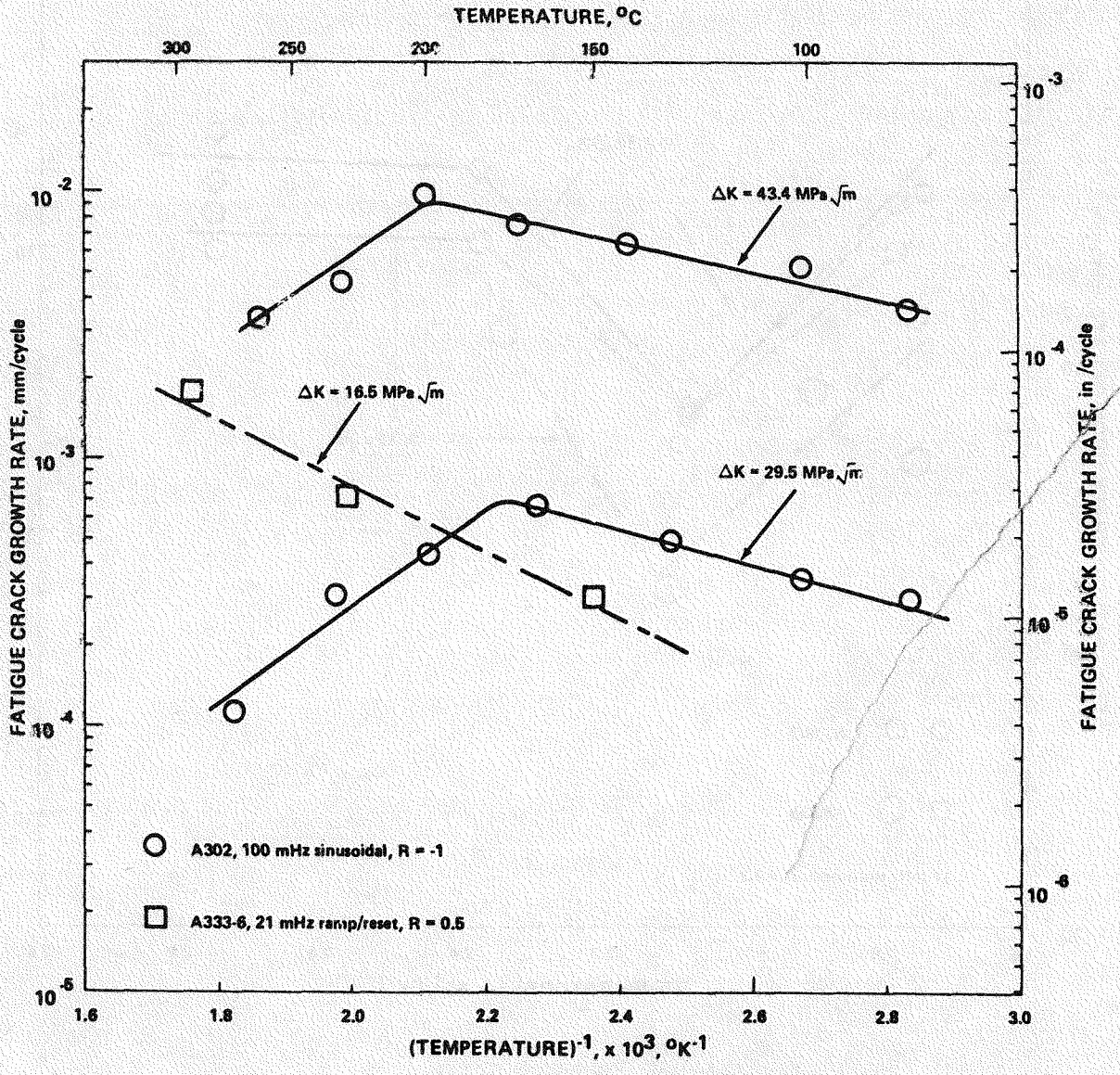

Fig. 9. Fatigue crack growth rates of A 302B and A 333-6 at specific values of ΔK vs. reciprocal temperature, for BWR environments. Data on A 302-B are from Kondo (Ref. 7) and on A 333-6 from Prater (Ref. 8).

5.3 Fractographic Studies

An extensive investigation of the fractographic features of the fatigue fracture surfaces was carried out in order to support discussion of the possible mechanisms which could account for the fatigue crack growth rates observed in this study. After the oxide identification was complete, attempts were made to remove the oxide using an ENDOX-based electrolytic method (Ref. 15). The ENDOX treatment successfully removed all the oxide from the surfaces of the two specimens tested at the higher temperature, and most of the oxide from the 93°C fatigue fracture surface, but had little effect on the oxide on the 149°C fatigue fracture surface. The implications of this difficulty are not understood in view of the fact that the oxide was identified as magnetite in all four cases. The fractographic observations are summarized in Table 3. Fractographs which are representative of these fatigue fracture surfaces are included as Figs. 10-18.

Table 3. Summary of Fractographic Observations on Fatigue Fracture Surfaces at Four Temperatures

Spec Q71-3 - air at 288°C (550°F)

- Ductile striations
- Transgranular propagation
- Some microcracks at high ΔK

Spec. Q71-24 - 93°C (200°F)

- Quasi-cleavage-like
- Some fan-shaped features
- No ductile or brittle striations
- No terraces
- Few microcracks

Spec. Q71-17 - 149°C (300°F)

- Similar to Q71-24 (above)
- More fan-shaped features

Spec. Q71-15 - 204°C (400°F)

- No quasi-cleavage-like features
- Ductile striations at low ΔK
- Poorly-defined brittle-like features at high ΔK
- Larger quantity of fan-shaped features
- Some terracing

Spec. Q71-22 - 288°C (550°F)

- Brittle-like features at all ΔK
- Few microcracks
- Some ductile striations at high ΔK, near bend-over

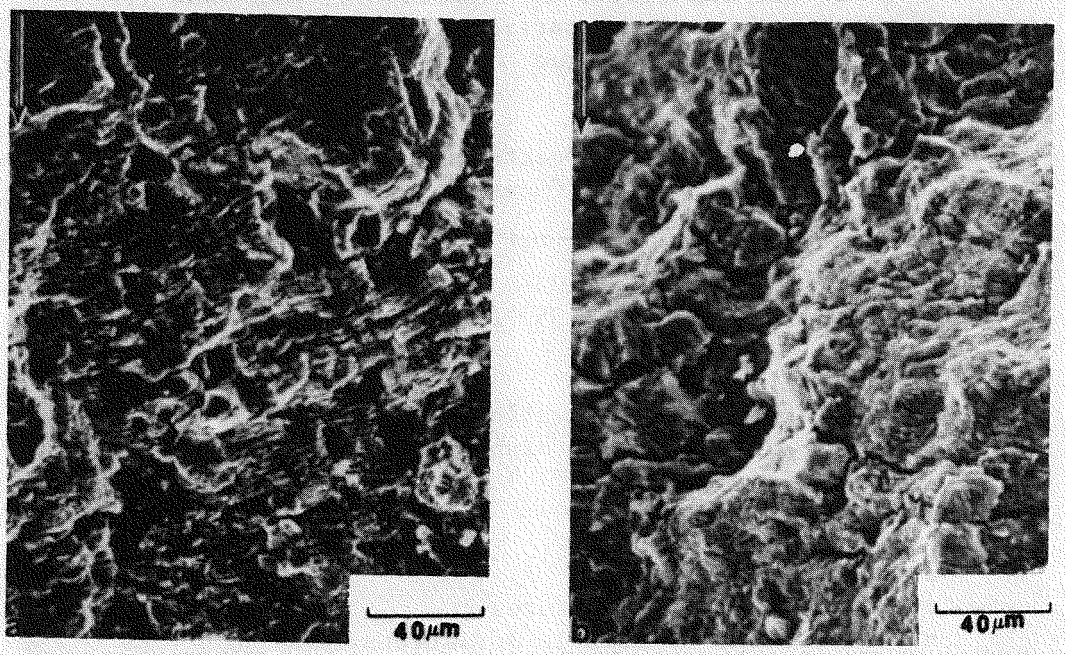

Fig. 10. Fatigue fracture surface of A 508-2 tested at 288°C in air environment. Growth direction indicated by the arrow. The values of ΔK were (a) 29.7 MPa $\sqrt{m}$ and (b) 44 MPa $\sqrt{m}$. Micrographs show that the failure mode for both specimens was transgranular with fatigue striations and extensive secondary cracking clearly visible in the high ΔK region.

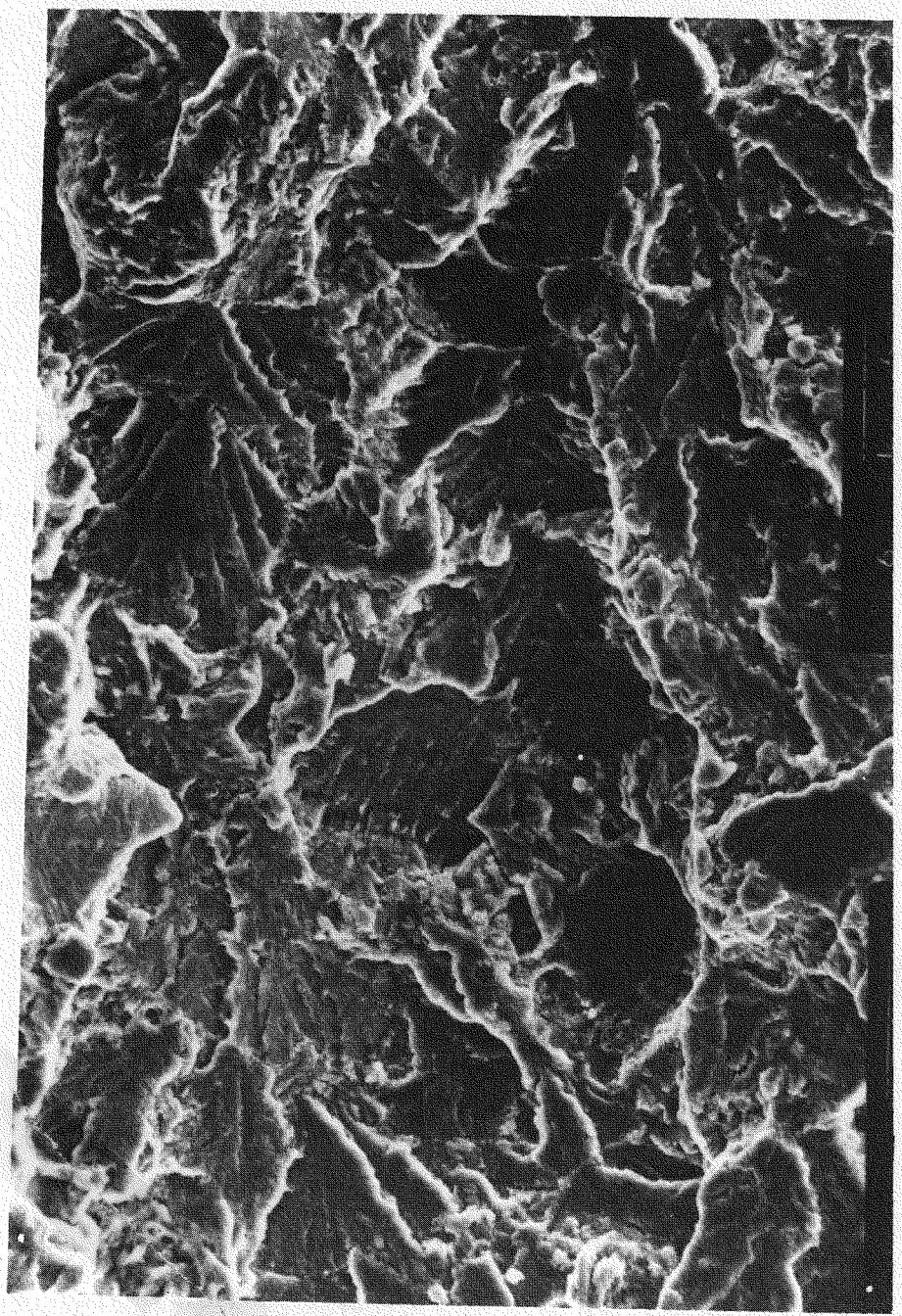

1000X

Fig. 11. Fatigue fracture surface of A 508-2 tested at 93°C in reactor-grade water. Growth direction indicated by the arrow. The value of applied ΔK at this crack length was 30 MPa $\sqrt{m}$. Note the quasicleavage typical features and the absence of microcracks.

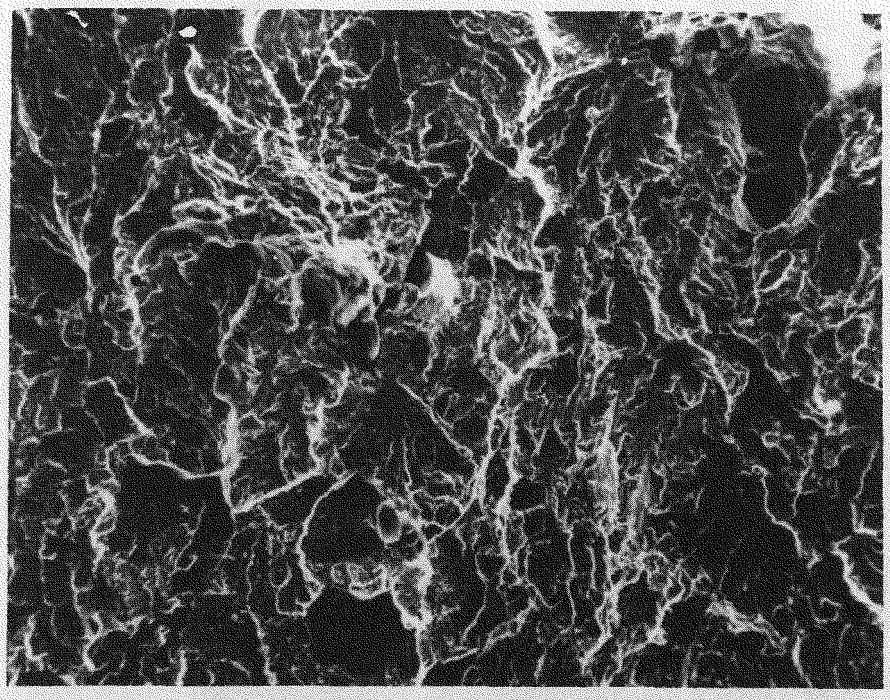

300X

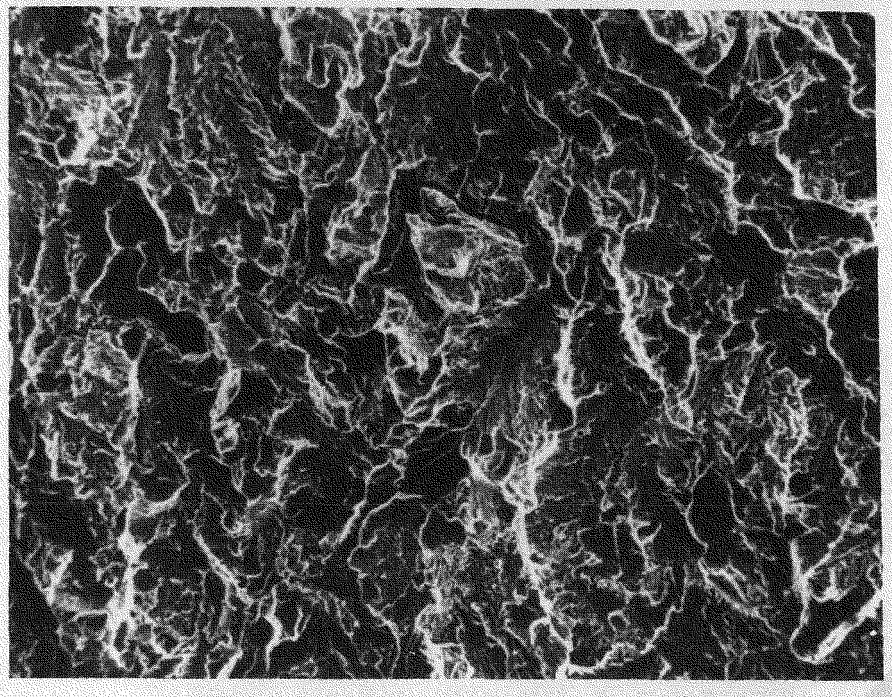

300X

Fig. 12. Fatigue fracture surface of A 508-2 tested at 93°C in reactor-grade water. Growth direction indicated by the arrow. The value of applied ΔK at this crack length was 40.5 MPa$\sqrt{m}$. Note the quasi-cleavage typical features, and the fan-shaped facets. At this Δ K level, a few randomly located microcracks can be found.

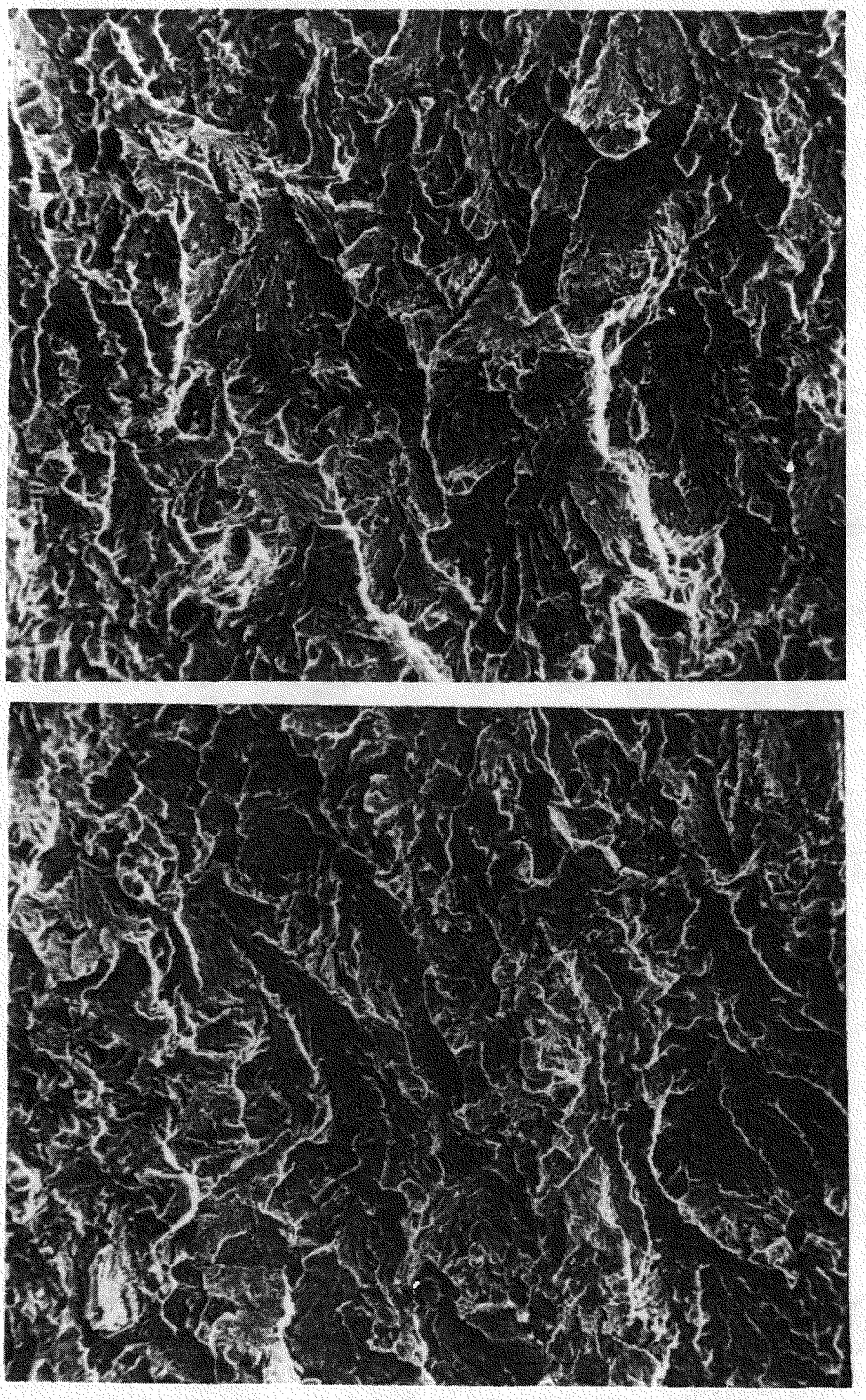

Fig. 13. Fatigue fracture surface of A 508-2 tested at 149°C in reactor-grade water. Growth direction indicated by the arrow. The value of applied ΔK at this crack length was 30.4 MPa $\sqrt{m}$. Although the oxide removal is quite incomplete, the presence of fan-shaped features and quasi-cleavage-like features can be seen easily.

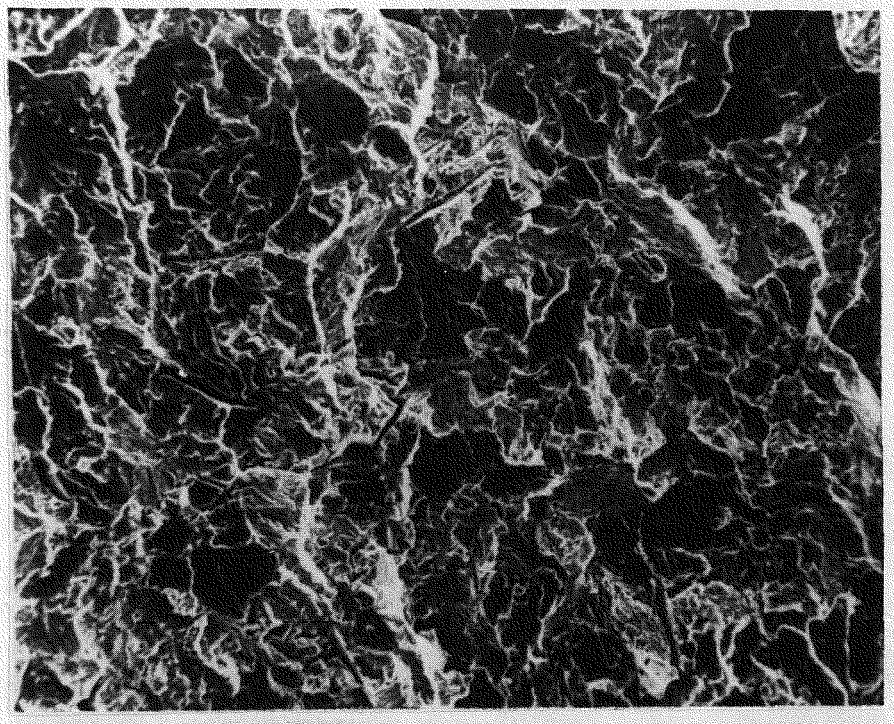

300X

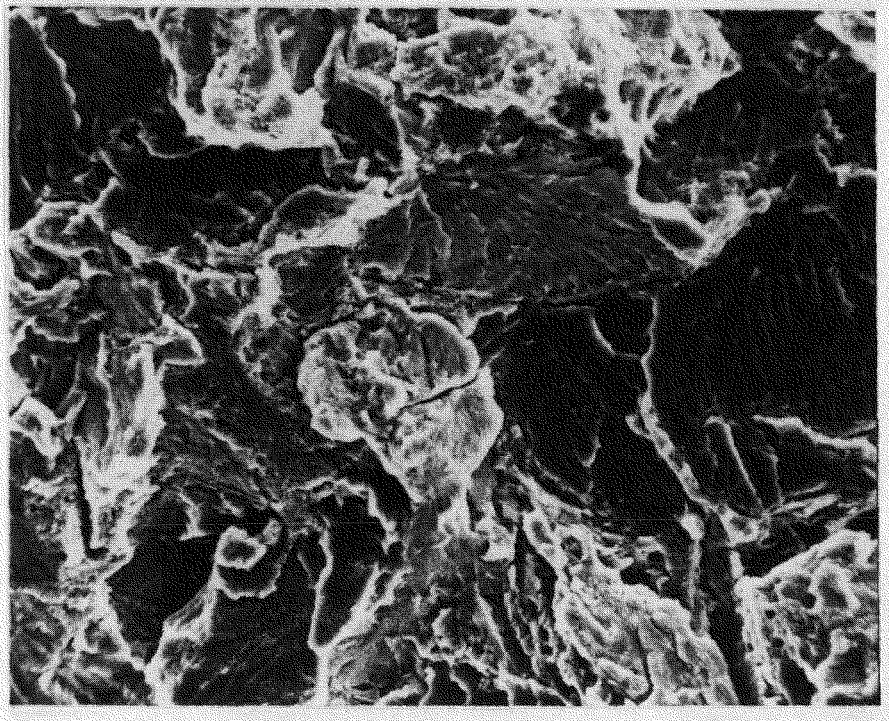

1000X

Fig. 14. Fatigue fracture surface of A 508-2 tested at 149°C in reactor-grade water. Growth direction indicated by the arrow. The value of applied ΔK at this crack length was 47 MPa $\sqrt{m}$. Figure 10b is a higher magnification of the lower-right section of Fig. 10a. The test concluded soon after this this ΔK level was achieved and the relatively small amount of oxide was more easily removed from the surface at this location than for the location of Fig. 9. Note some micro-cracking and fan-shaped features (a) and lack of striations (b) at this rather high ΔK value.

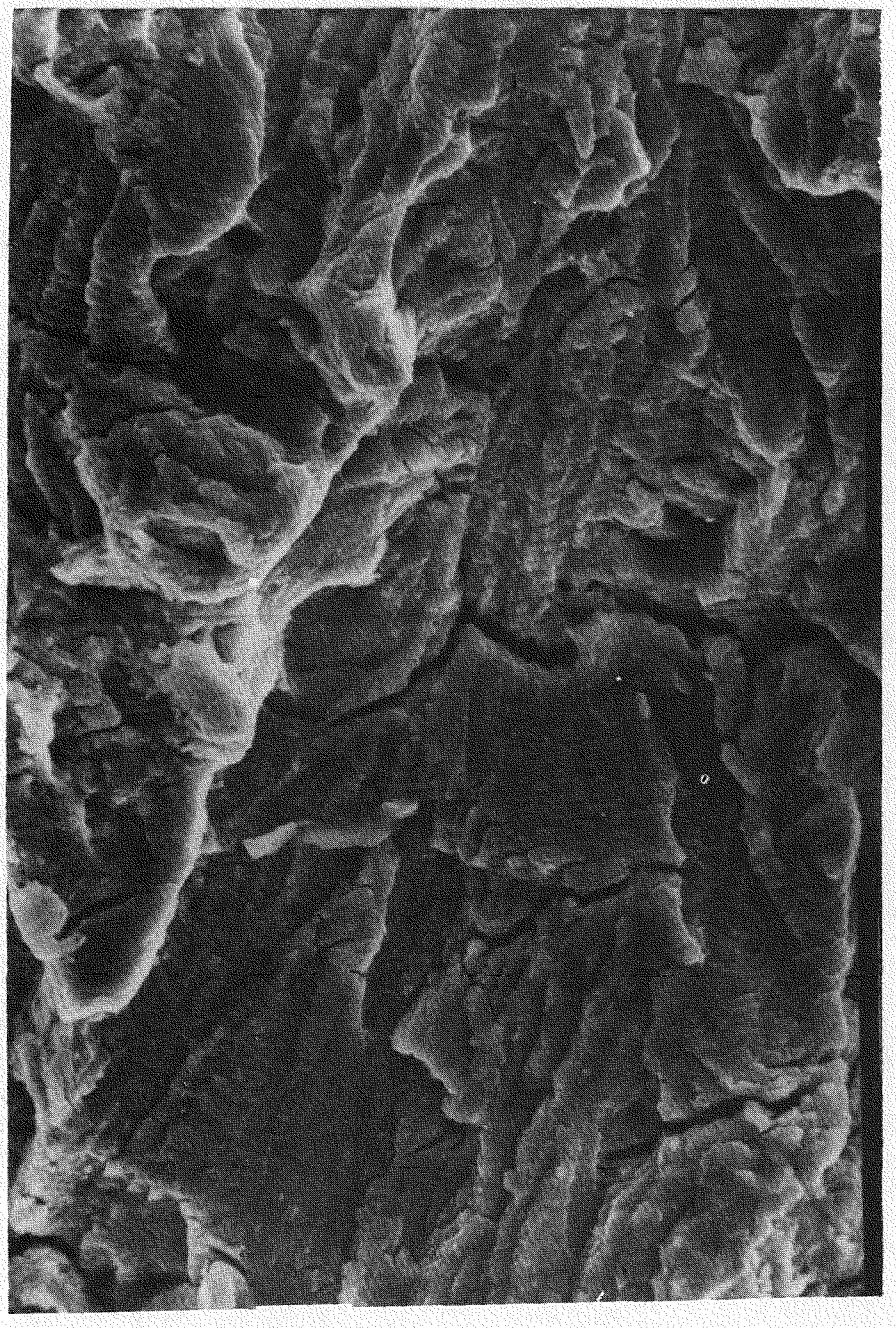

Fig. 15. Fatigue fracture surface of A 508-2 tested at 204°C in reactor-grade water. Growth direction indicated by the arrow. The value of applied ΔK at this crack length was 25 MPa$\sqrt{m}$. Note the ductile striations formed at this ΔK level.

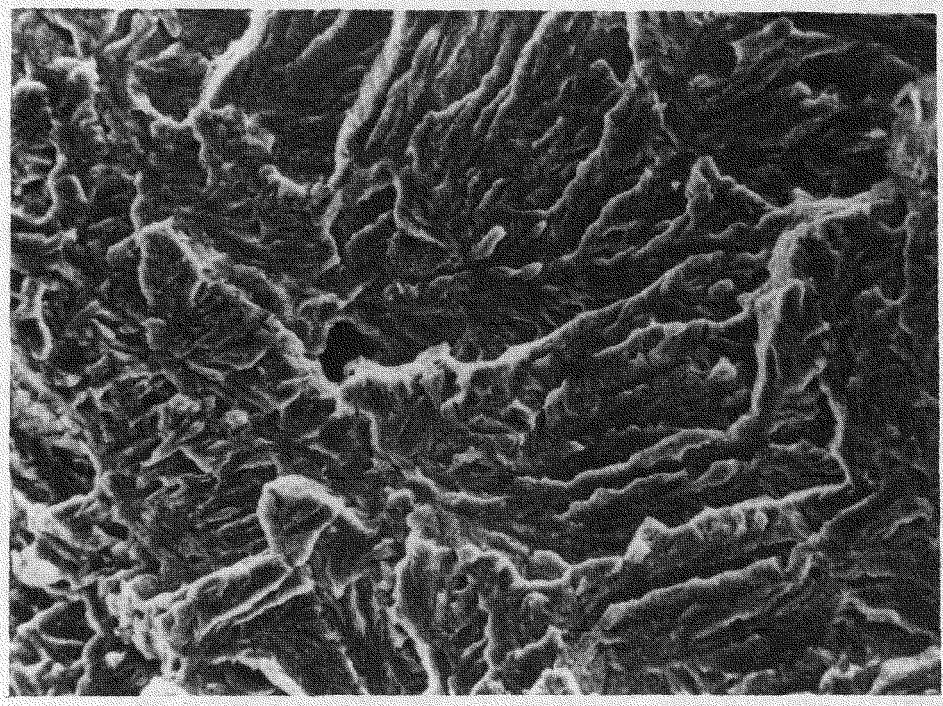

1000X

Fig. 16. Fatigue fracture surface of A 508-2 tested at 204°C in reactor-grade water. Growth direction indicated by the arrow. The value of applied ΔK at this crack length was 40 MPa $\sqrt{m}$. Note the character of the brittle-like fatigue fracture differs markedly from the quasi-cleavage-like failures in Figs. 10 to 13.

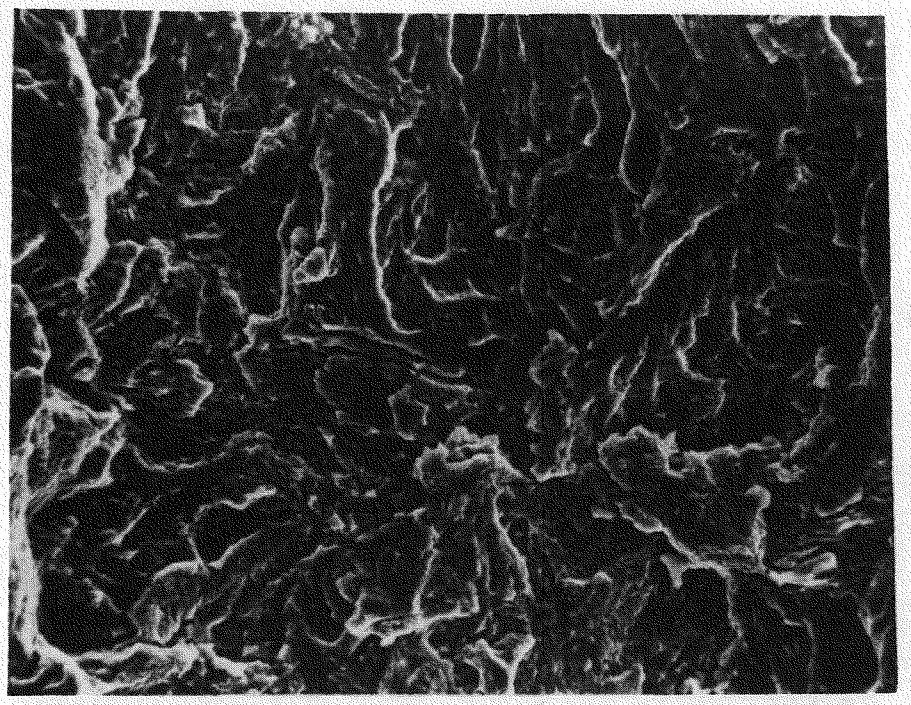

1000X

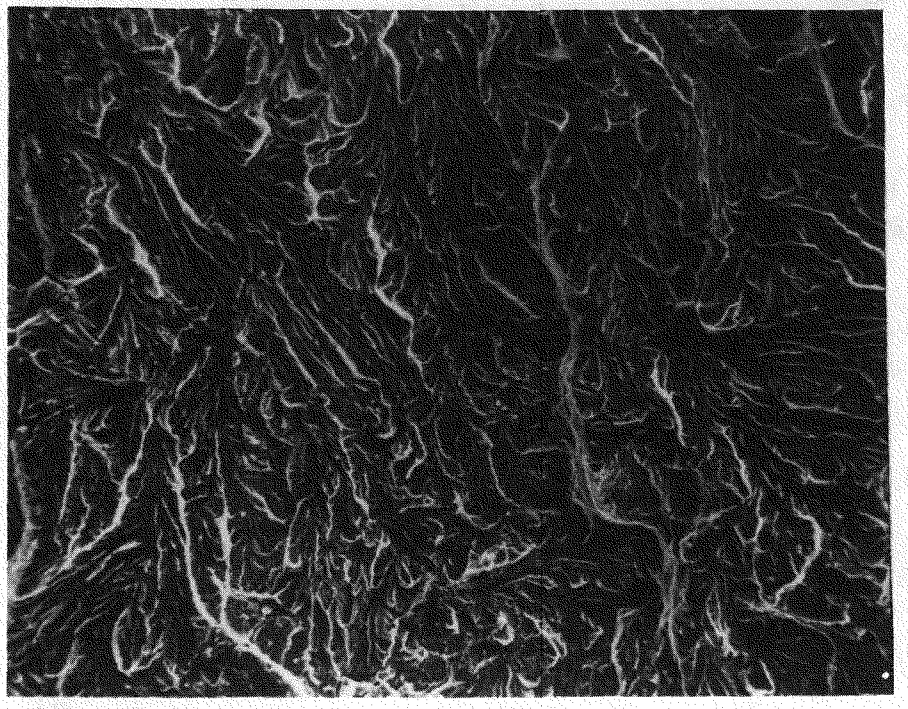

300X

Fig. 17. Fatigue fracture surface of A 508-2 tested at 288°C in reactor-grade water. Growth direction indicated by the arrow. The value of applied ΔK at this crack length was 30.3 MPa $\sqrt{m}$. Note the brittle-like character on the alluvial or fan-shaped facets.

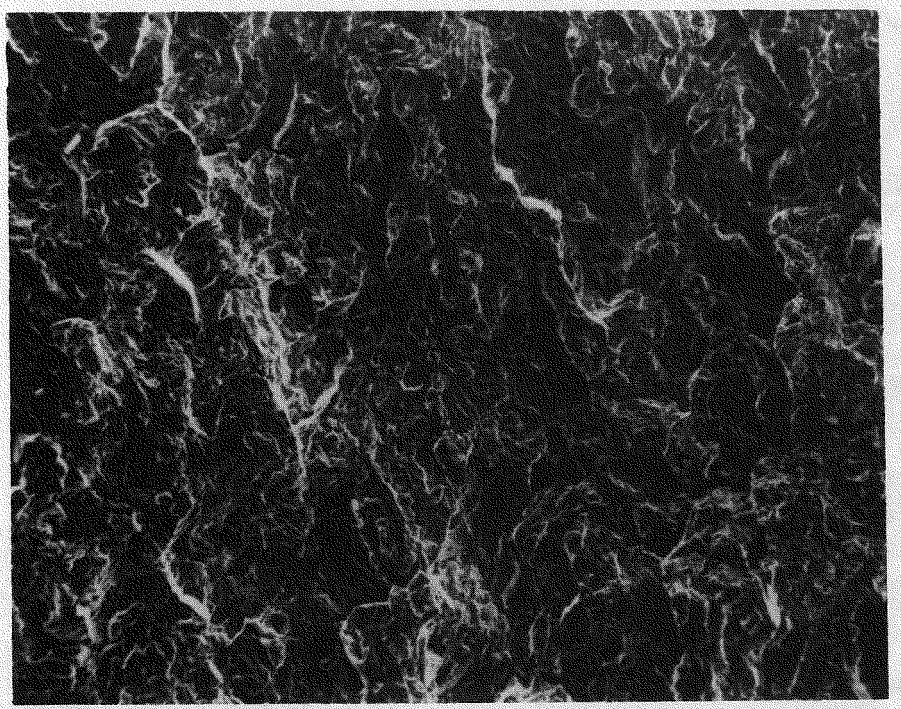

100X

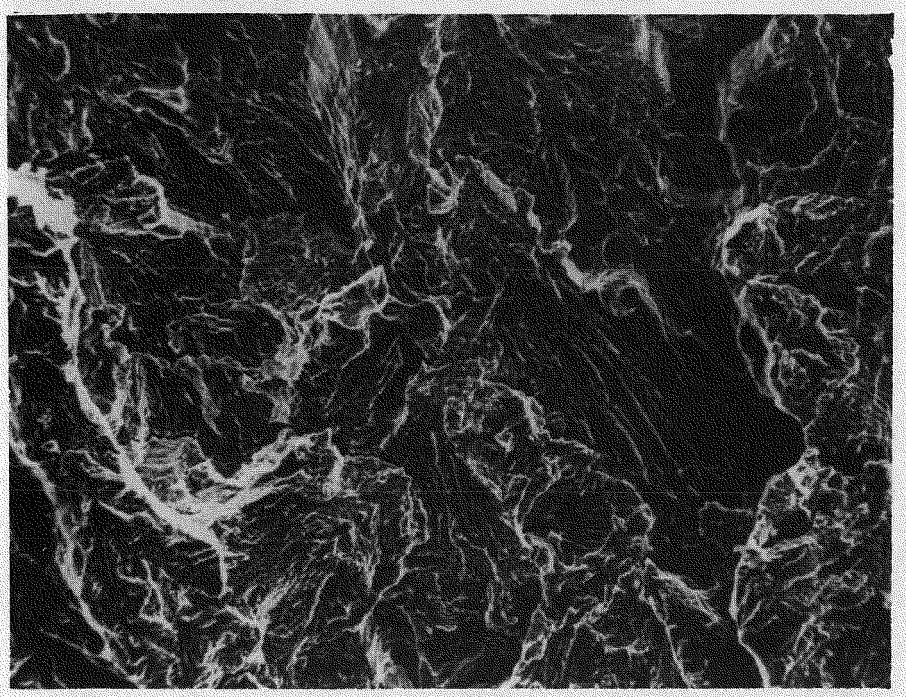

300X

Fig. 18. Fatigue fracture surface of A 508-2 tested at 288°C in reactor-grade water. Growth direction indicated by the arrow. The value of applied ΔK at this crack length was 51 MPa $\sqrt{m}$. Ductile striations are visible on some of the fan-shaped facets at center and on left side.

6. SUMMARY AND CONCLUSIONS

The results of this study can be summarized as follows:

- Fatigue crack growth rates in this heat of A 508-2, at temperatures of 93°C, 149°C and 288°C reside near the ASME default line for surfaces flaws for which R ≤0.25.

- Fatigue crack growth rates in this heat of A 508-2 at 204°C reside near the default line for R ≤0.25 for low ΔK values (<25 MPa $\sqrt{m}$), but then exhibit a nearly Δ K-independent, "plateau" behavior.

- The oxide on the fatigue fracture surfaces has been identified as magnetite for all temperatures.

- The fracture surface consists of quasi-cleavage-like and some fan-shaped features at the two lower test temperatures. Some brittle-like features were observed at the two higher test temperatures. Ductile striations were found at high ΔK values for the 288°C test, and at low ΔK values for the 204°C test.

Based on this information - growth rates, oxide identification, and fractography - it is difficult to determine whether more than one micromechanism is responsible for the environmental assistance observed in these results. The facts that growth rates at the two lowest temperatures are virtually identical and are linear on the conventional log-log plot, and that the oxide on both specimens was difficult to remove, indicate that these tests should stand by themselves. The presence of ductile and brittle striations on the two high temperature specimens, and the fact that growth rates on both are non-linear, suggest that those two tests should stand by themselves.

On the other hand, the fact that the oxides are magnetite at all temperatures, and that the electrochemical potentials are in the -650mV to -850mV (vs. SHE) range at all temperatures greater than 150°C implies that the electrochemical conditions resulting in corrosion are nominally the same for all the tests. The gradual increase in fan-shaped features with increasing temperature suggests a common mechanism, with a monotonic temperature dependence. In view of these observations, it is impossible to assert that there is just one active mechanism responsible for the environmental assistance over the whole temperature range. It appears that a second mechanism is also active at the lower temperatures, phasing out at about 180°C. At this temperature, the growth rates decrease drastically, then increase as the kinetics of the first mechanism respond to the increase in temperature. The presence of fan-shaped and brittle-like, quasi-cleavage features at all temperatures, and the fact that hydrogen evolution occurs at the pH level (~6.5) and corrosion potential of the test environment suggests that the overall mechanism will be some form of hydrogen-assisted fatigue crack growth.

REFERENCES

1. Section XI of the ASME Boiler and Pressure Vessel Code, Rules for In-service Inspection of Nuclear Power Plant Components, ANSI/ASME-BPV-XI-1, American Society of Mechanical Engineers, New York, issued annually.

2. Bamford, W. H., "Technical Basis for Revised Reference Crack Growth Rate Curves for Pressure Boundary Steels in LWR Environment", J. Press. Vessel Tech. 902, pp. 433-442.

3. Bamford, W. H., Moon, D. M., and Ceschini, L. J., "Environmentally Assisted Crack Growth in Light Water Reactor Materials - Annual Technical Progress Report, Fiscal Year 1981", Westinghouse Electric Corporation, P. O. Box 355, Pittsburgh, PA 15230, 1981.

4. Slama G., and Rabbe, P., "French Approach and Results in Cyclic Crack Growth" Proceedings of the 5th SMIRT Post-Conference Seminar, Paris, France, Aug. 1981, pp. 311-325.

5. Cullen, W. H. et al., "Fatigue Crack Growth of A508-2 Steel in High-Temperature, Pressurized Reactor-Grade Water", USNRC Report NUREG/CR-0969, 1979.

6. Cullen, W. H. et. al., "Fatigue Crack Growth Rates of Irradiated Pressure Vessel Steels in Simulated Nuclear Coolant Environment", J. Nuclear Materials 96, 1981 pp. 261-268.

7. Ford, F. P., "Mechanisms of Enviornmental Cracking in Systems Peculiar to the Power Generation Industry," EPRI Report NP-2589, Electric Power Research Institute, 3412 Hillview Ave., Palo Alto, CA 94304, Sept. 1982.

8. "Prediction of Enviornmental Crack Growth in Nuclear Power Plant Components - Semiannual Technical Progress Report No. 1, July 1982," Mager, T. R., Sabol, G. P. and Slama, G., Principal Investigators, Available from Electric Power Research Institute, 3412 Hillview Ave., Palo Alto, CA 94304.

9. Kondo, T. et. al., "Corrosion Fatigue of ASTM A302B Steel in High Temperature Water-the Simulated Nuclear Reactor Environment" in Corrosion Fatigue: Chemistry, Mechanics and Microstructure, NACE-2, eds. O.Devereux et al., National Association of Corrosion Engineers, Houston, TX, 1973 pp. 539-556.

10. Prater, T.A., and Coffin, L. F. "Crack Growth Studies on a Carbon Steel in Oxygenated High-Pressure Water at Elevated Temperatures", in Proceedings of Specialists' Meeting on "Subcritical Crack Growth," 13-15 May, 1981, International Atomic Energy Agency, 1981, pp. 640-654.

11. Atkinson, J. D., Cole, S. T. and Forrest, J. E., "Corrosion Fatigue Mechanisms in Ferritic Pressure Vessel Steels Exposed to Simulated PWR Environments" Proceedings of Specialists' Meeting on "Subcritical Crack Growth", 13-15 May, 1981, International Atomic Energy Agency, 1981, pp. 459-483.

12. Cullen, W. H., "The Effects of Waveform, Frequency and Temperature on Fatigue Crack Growth in RPV Steels", in Aspects of Fracture Mechanics in Pressure Vessels and Piping, PVP-Vol. 58, Amer. Soc. Mech. Engineers, 1982, pp. 303-312,

13. Bamford W. H. and Moon, D. M. "Some Mechanistic Observations on the Crack Growth Characteristics of Pressure Vessel and Piping Steels in PWR Environment", Paper No. 222, Corrosion, 1980 36(6).

14. MacDonald, D. D., et al., "The Effects of BWR Deaeration on the General and Localized Corrosion of Plain Carbon and Low Alloy Steels EPRI Project T115-5" EPRI Progress Report 1 July - 31 Dec. 1980, Electric Power Research Institute, Palo Alto, CA 94303.

15. Yuzawich, P. and Hughes, C. W., "An Improved Technique for Removal of Oxide Scale from Fractured Surfaces of Ferrous Materials", Practical Metallography, 15, 1978, pp. 184-195 .